3400—Forest Health Protection
Technical Report 0734–2815

Determining How Much Weight Emerald Ash Borers Can Carry in Flight

Keith Windell
Project Leader

Jim Kautz
Photographic Technologist

USDA Forest Service
Technology and Development Program
Missoula, MT
September 2007, Revised January 2009

Table of Contents

Highlights

- The emerald ash borer (*Agrilus planipennis*), an exotic beetle from Asia, is a recently introduced insect pest.
- Tiny transponders have been used to track the spread of other introduced insects, but the emerald ash borer, which weighs just 50 milligrams or so, is much smaller.
- The heaviest weight a female emerald ash borer could carry in flight was 16 milligrams, 38 percent of its body weight.
- High-speed cameras showed that the fastest female emerald ash borer flew 5.4 feet per second for 72 inches with a 9.9 milligram-load, 18 percent of its body weight.

Introduction

The emerald ash borer (*Agrilus planipennis*, referred to as borer in this report), an exotic beetle from Asia, is a recently introduced pest that has become established in southeastern Michigan and Windsor, Ontario. Newly established populations of borers have also been detected in other areas of southern Michigan and in several locations in Ohio. Infested nursery trees have been found in Maryland and Virginia.

Females lay their eggs in crevices on the trunks or branches of ash trees. After the eggs hatch, the larvae chew through the bark and into the cambium of the tree. Their S-shaped feeding galleries end up cutting off the flow of nutrients and water to the tree. Many trees lose a third to half of their leaves within 2 years and the trees may die within 3 to 4 years. After borers emerge from the galleries, they fly to other ash trees, where they feed on leaves.

One way to help predict the borer's spread would be to track individual beetles in the wild, as had been done with Asian longhorn beetles. The tiny transponders used to track those beetles are too large for the emerald ash borer, which may weigh just 50 milligrams.

Harmonic radar and Schottky diode-based transponders are being considered for borers. It appears that a tiny transponder may have to be developed specifically for this borer. The transponder must not significantly affect the natural flight characteristics of the borer or its true range potential will not be known.

The Missoula Technology and Development Center (MTDC) was asked to work with Therese Poland's research entomology staff at the North Central Research Station in East Lansing, MI. MTDC used a high-speed video camera to determine how weights glued to the borers affected the average flight speed right after a borer took off and for as long as the camera could record its flight.

Methods

The authors traveled to the North Central Research Station and set up a video studio (figure 1) to record the borer's flights. The studio was in a 20- by 30-foot room. Windows and vents were covered with plastic, which prevented the borers from escaping, but made the room quite hot. A white sheet was attached to one corner of the room and two large mirrors were clipped together. The mirror assembly was positioned touching the back wall such that the angle formed between the mirror surface and the back wall was 135 degrees.

Figure 1—The video studio where the emerald ash borer flights were filmed.

Video files were used to determine the borer's *X* and *Y* pixel position on an imaginary vertical plane, *Ip*, a known distance from the camera (figure 2). The mirror was used to generate a reflected image of the borer. A set of pixel coordinates for this reflected image was also recorded on video. Formulas were derived to map the two pairs of 2-D coordinates (generated by video analysis software) into 3-D space (appendix E).

Figure 2—The high-speed camera used to film the flights.

A steel ruler (with high and low marks) was placed in the borer's flight area (figure 3) to serve as a calibration marker. It allowed a scale factor to be determined so the 2-D pixel coordinates could be correlated to the actual distances from the origin of the imaginary plane, *Ip*, and the camera's focal point. The steel ruler was placed at different locations in the camera's viewing area so the accuracy of the analysis could be checked later. A borer was placed on a launch stick in the middle of the room behind the imaginary plane, *Ip*. The video camera recorded the borer's change in position and in its reflected position throughout the flight.

Figure 3—Establishment of a calibration position.

To determine how well a borer could fly with extra weight, research station technicians glued weights to the top of the borer's thorax. Gluing the weights farther back would have interfered with the borer's wings. A weight glued to the bottom of the borer would have dragged on the ground. Small pieces of plastic and bits of paper clip were used as weights (figures 4 and 5). Although we were attempting to determine how much weight the borer could carry while flying, the transponder's bulk and the antenna's design will also affect the borer's flight.

Weights ranged from about 1 milligram to 20 milligrams. Rubber cement added an additional 0.5 to 1 milligram. Permanent glues are available that weigh less, but we wanted the flexibility to remove one weight and attach another. We focused on female borers because they venture out and lay eggs. Female borers also are much larger than males. Transponders may be very difficult to mount on the male borers.

Figure 4—An emerald ash borer with a plastic weight.

Figure 5—An emerald ash borer with a metal weight.

The borers used in the tests were reared at the station's lab and hatched out from May 23 to May 26. The flight tests were on June 1 and 2. Fresh ash leaves were placed on a bright light above the launching stick. The plan was to entice the borers to fly up to the leaves. The leaves seemed to serve as an incentive because several borers went to the light or the ash leaves. Once a borer was placed on the launching stick, the waiting game started. Some took off immediately (figure 6), while others fell off the launching stick or just stayed there.

Figure 6—An emerald ash borer in flight.

The video was captured with a Photron FASTCAM Ultima APX high-speed camera with one megapixel ultrahigh sensitivity imaging sensor. The size of the viewing area (face of the imaginary plane *Ip*) was determined by the imaging sensor and was set at 1,024 pixels wide and 512 pixels high. The camera's frame rate was 250 frames per second. File sizes were typically in the 400- to 700-megabyte range for a 1.0- to 1.5-second flight. The size of the "3-D space" filmed was about 33 inches tall by 66 inches wide by 40 inches deep. Half of the width was the reflected image off the mirror.

Two sets of raw data files were saved for each flight, one .avi file for general viewing and a .cih file used by proprietary software to perform the motion analysis. The .cih files were turned into two sets of 2-D pixel coordinates using the camera's Photron Motion Tools software package. Each location of interest had to be individually digitized. The borer appeared as a cluster of dark and light pixels. One of the pixels had to be selected as the representative center of mass.

The coordinate system provided in the Photron Motion Tools software required that the origin of the imaginary plane *Ip* be in the upper left-hand corner of the video image. A scale factor was applied to the pixel coordinates (based on calculated pixel/height measurement ratios on the face of the imaginary plane). To determine the borer's distance from the origin of the imaginary plane, *Ip*, a large mirror was set up, allowing a video camera across the room to view the borer and its reflection in the mirror simultaneously.

The software could only track one object at a time, so each flight and the reflection of that flight had to be digitized separately. The coordinates for each point during flight and the reflection of that point were spliced together by matching the time codes to create a matched set of 2-D pixel coordinates that were saved as Excel files. These two sets of 2-D pixel coordinates were turned into 3-D spatial coordinates using formulas derived in appendix E.

The following geometric approach is illustrated in figure 7:

1. An equation was determined for the line L_1 passing through the camera's focal point and the borer's reflected image, labeled "A," on the imaginary plane, *Ip*. The origin of the reference coordinate system was on the imaginary plane, *Ip*.
2. An equation for the mirror surface was determined by referencing the measured room layout and its relationship to the origin of the imaginary plane, *Ip*.
3. The intersection of line L_1 and the mirror's surface was calculated. This point, labeled "R," represented the location of the borer's reflected image on the mirror surface in relation to the origin of the imaginary plane, *Ip*.
4. An equation was determined for the reflected line from the point on the mirror's surface back toward the borer.
5. An equation was determined for the vertical plane that contains the focal point of the camera and the borer's projected image on the imaginary plane, *Ip*, labeled "B." This vertical plane also passes through the borer.
6. The intersection of the reflected line coming off the mirror surface and the vertical plane passing through the camera's focal point and the borer was determined. This point, labeled "P," was the approximate 3-D spatial location of the borer.

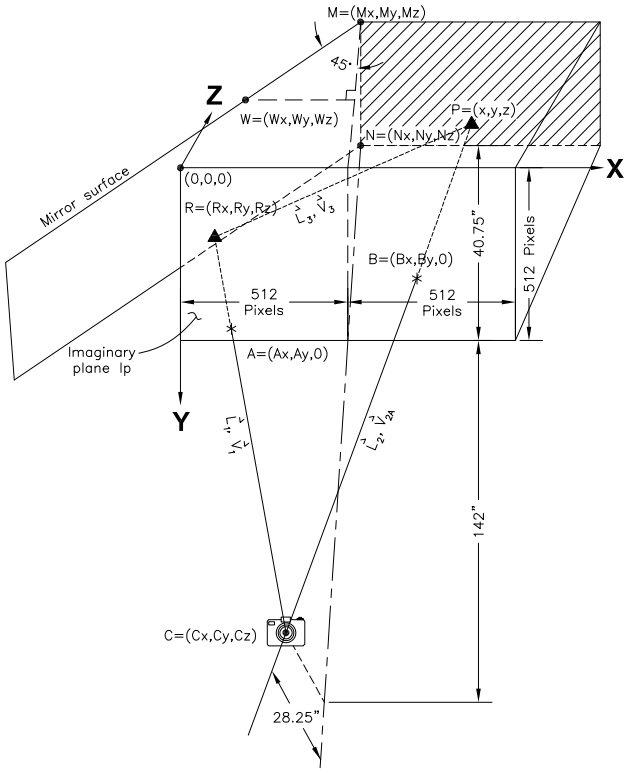

Figure 7—This diagram shows the geometry used when transforming a matched set of two 2-D coordinates into a 3-D spatial coordinate.

The incremental distances of the borer from the launching stick were calculated, summed, and divided by the total time of flight (using the video time code) to determine the borer's average speed. All computations were done in an Excel spreadsheet.

To get a handle on the accuracy of this approach, the relative coordinates for the object's location had to be transformed to a coordinate system in which the origin was at the base of the camera directly below the focal point of the lens. This was done to allow comparison of the

measured locations of numerous calibration points established earlier with the positions calculated from the derived equations.

Possible sources of experimental error included imperfect mirror alignment (a single mirror would have been better), imperfections in the mirror's surface, imperfect alignment of the calibration stick, and imperfect measurements of the room's dimensions and the positions of the calibration sticks. Imperfect mirror alignment did not allow as precise a geometric solution as was originally envisioned. Rather than determining the intersection of two lines to locate the borer's final position, the intersection of a line and a vertical plane had to be used (see appendix E for more information).

Appendix F includes the comparison of the calculated values to the measured values. The calculated position of a calibration point is arrived at by taking the pixel location of the object and its reflection on the imaginary plane, *Ip*, and using a system of geometrically derived equations to determine the object's position somewhere behind the imaginary plane, *Ip*. The actual position of a calibration point was accurately measured during the initial layout of the test room.

The largest deviation from the measured calibration points (with no known errors) to the centerline in the middle of the room (*X*-coordinate) was 0.25 inch (0.79 percent). The *X*-coordinate for calibration point 4 was excluded because it appears to have been about 0.4 inch off its intended centerline position. This may have been because it was in the corner of the intersection of the mirror and the back wall of the room. The percent error for the *X*-coordinate of calibration point 3 was 6.6 percent. This point was also excluded because of the mathematical approach used to avoid dividing by zero.

The largest deviation from the measured calibration points in the vertical position (*Y*-coordinate) was 0.28 inch. The largest percent error was 1.3 percent. The largest deviation from the measured calibration points (with no known errors) from the base of the camera (*Z*-coordinate) was 0.82 inch (0.58 percent). Again, calibration point 4 was excluded because it was not positioned on the centerline. Given that some of these test positions were as far as 180 inches away from the camera's focal point, this experimental approach resulted in a 1 percent error (or less) when the straight-line distances were compared.

Results

Appendix A includes basic information about each flight. Appendix G, "Calculated Results for Plotting," includes the results of calculations to determine the borer's average speed for these short flights, graphed in figures 8 and 9.

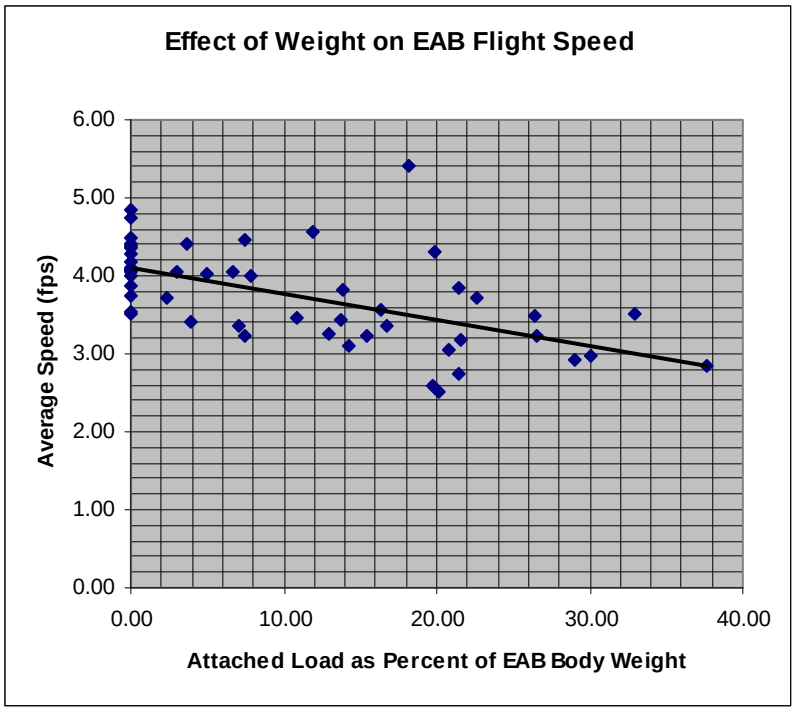

Figure 8—The effects of weight on a borer's flight speed, based on the weight of the attached load as a percent of the borer's weight.

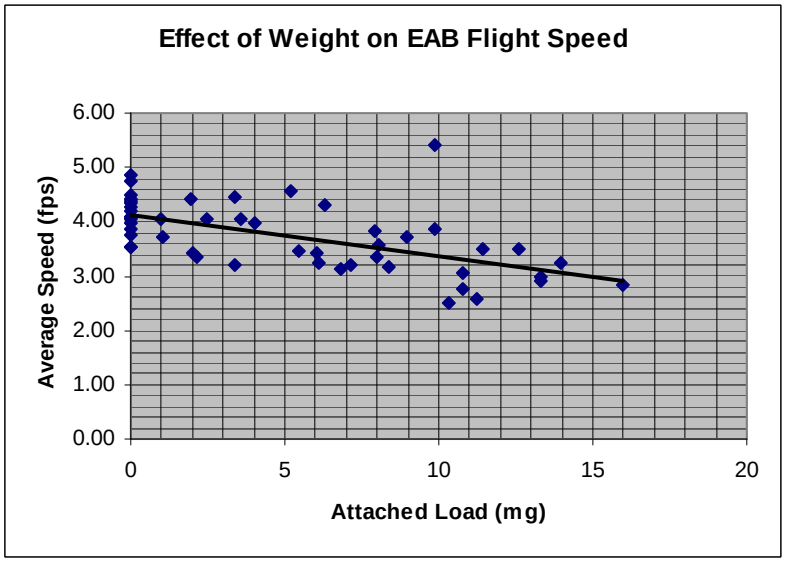

Figure 9—The effects of the weight of an attached load on a borer's flight speed.

The information in appendixes A and G is the basis for the following observations:

- Plotted flight data consisted of a relatively small sample size of 34 female borers with weights attached and 17 female borers without weights. Twenty-five additional flights of female borers were not included in the sample because the borers didn't fly

long enough or because of technical difficulties. Five unweighted males were also tested with one of the male flights having to be excluded.

- Females flew for an average of 1.1 seconds before they left the observation area.
- Males were smaller (average weight 25.8 milligrams) than the 17 unweighted females (average weight 43.5 milligrams) and slightly faster (average flight speed 4.31 feet per second for males compared to 4.15 feet per second for the unweighted females). The males may be too small to fly with a transponder.
- The heaviest weight a female borer could carry while flying was 16 milligrams, about 38 percent of its body weight (flight No. 34).
- The fastest female borer carrying a weight flew an average of 5.4 feet per second over a 72-inch flight path with a 9.86-milligram load (flight No. 57B). This borer hatched on May 23 and flew on June 2, making it one of the oldest borers we studied. It weighed 54.2 milligrams before weight was added and carried a load that was 18 percent of its body weight.
- Even borers with no weight (flights Nos. 4, 11, and 68) sometimes dove to the ground. Perhaps the borers were tired or their wings had been glued together by mistake.
- The 6.22-milligram and 6.91-milligram weights used in flights Nos. 44B and 60 were too heavy. The borer was just able to hover before crashing to the floor.
- If a flight speed reduction of 10 percent is considered acceptable, then the transponder, antenna, and glue probably need to weigh less than 2 milligrams (see graphs).
- If a flight speed reduction of 25 percent is considered acceptable, the transponder, antenna, and glue may weigh up to 5.75 milligrams for a mature female borer (perhaps as much as 10 milligrams for an exceptionally healthy female borer). Even the 5.20- and 5.46-milligram weights used during flights Nos. 45 and 43 taxed mature females by making them hover before they flew up and away.
- The weight limit for a 25-percent speed reduction corresponds to 14 percent of the borer's weight.
- The incremental average speeds right after the borer leaves the launch stick are much faster than average speeds indicated in earlier published flight mill tests. Because of the possible sources of error in this experimental approach and the extremely short flight duration recorded on videotape, caution should be exercised when considering the accuracy of these calculated speeds and whether borers could maintain them for very long. It may be safer to focus on the relative drop in performance based on the attached weight rather than to assume that the borer can maintain those speeds. The borers we tested eventually landed in the room, but there's no way to know whether they landed because of fatigue or because they couldn't leave the room.

Recommendations

- Track borers over longer distances, if possible. (The current test does not address fatigue during extended flights).
- Conduct future flight tests in a larger room so that the camera's focal point can be farther away, reducing lens-induced error. Use a telephoto lens as needed.

- Experiment with reducing the frames per second being recorded to limit the data being stored and to increase the length of time data can be collected. (Although conventional digital video cameras may record 30 to 60 frames per second, they may not provide adequate resolution. The Photron Motion Tools 3-D photo analysis software requires high camera resolution).
- Use at least a two-camera system with canned 3-D conversion software to reduce the time needed to process the data and increase confidence in the results (software must have autotracking feature).
- Increase the sample size.
- Test bulky weights to determine how large the transponders can be before they interfere with a borer's movements.
- Test simulated antennas to determine how they may affect a borer's wing movements.

Appendix A—Flight Data

Flight Information

FLT No.	Hatch date	Borer wt. (grams)	Total wt. (grams)	Load wt. (grams)	Loc.	Sex	WL	Flight date	Notes
1	25-May	0.0353	NW		CFP	F		1-Jun	
2*	25-May	0.0412	0.0624	0.0212	CFP	F	TT	1-Jun	Borer launched from hand, crashed, nose dive down
3*	25-May	0.0452	0.0625	0.0174	CFP	F	TT	1-Jun	Borer launched from hand, crashed, nose dive down
4*	25-May	0.0311	NW		CFP	F		1-Jun	Nose dive down
5	25-May	0.0436	NW		CFP	F		1-Jun	
6	24-May	0.0529	NW		CFP	F		1-Jun	
7*	24-May	0.0246	NW		CFP	F		1-Jun	Borer in midair when video footage starts
8	24-May	0.0332	NW		CFP	F		1-Jun	
9	25-May	0.0428	NW		CFP	F		1-Jun	
10	25-May	0.0363	NW		CFP	F		1-Jun	
11*	25-May	0.0458	NW		CFP	F		1-Jun	Fell off stick to ground

12	24-May	0.0446	NW		CFP	F		1-Jun	
13	24-May	0.0410	NW		CFP	F		1-Jun	
14	25-May	0.0530	NW		CFP	F		1-Jun	
15	25-May	0.0340	NW		CFP	F		1-Jun	
16	25-May	0.0406	NW		CFP	F		1-Jun	
17*	25-May	0.0484	NW		CFP	F		1-Jun	Flew out left side of mirror quickly
18	23-May	0.0469	NW		CFP	F		1-Jun	
19	23-May	0.0532	NW		CFP	F		1-Jun	
20	23-May	0.0490	0.0515	0.0025	CFP	F	TT	1-Jun	
21*	23-May	0.0515	0.0557	0.0042	CFP	F	TT	1-Jun	Flew straight to wall and landed
22	23-May	0.0272	0.0293	0.0021	CFP	F	BA	1-Jun	
23*	24-May	0.0392	0.0410	0.0019	CFP	F	TT	2-Jun	Went down to ground
24*	24-May	0.0337	0.0358	0.0021	CFP	F	TT	2-Jun	Never flew
25	25-May	0.0333	0.0343	0.0010	CFP	F	TT	2-Jun	
26_25A	24-May	0.0455	0.0465	0.0011	CFP	F	TT	2-Jun	Flight 26 was originally designated flight 25A.
27	24-May	0.0449	0.0483	0.0034	CFP	F	TT	2-Jun	

28*	24-May	0.0477	0.0561	0.0085	CFP	F	TT	2-Jun	Weight fell off at start of flight
29	24-May	0.0386	0.0470	0.0084	CFP	F	TT	2-Jun	
30	25-May	0.0459	0.0558	0.0098	CFP	F	TT	2-Jun	
31*	25-May	0.0443	0.0576	0.0133	CFP	F	TT	2-Jun	Flew to wall
31A	25-May	0.0443	0.0576	0.0133	CFP	F	TT	2-Jun	
31B*	25-May	0.0443	0.0576	0.0133	CFP	F	TT	2-Jun	Nose dive to ground
32	24-May	0.0459	0.0593	0.0133	CFP	F	TT	2-Jun	Long flight
33*	25-May	0.0471	0.0574	0.0103	CFP	F	TT	2-Jun	Long flight, no video
34	24-May	0.0424	0.0584	0.0160	CFP	F	TT	2-Jun	
35A*	24-May	0.0505	0.0702	0.0197	CFP	F	TT	2-Jun	Borer released from hand rather than placed on stick
35B*	24-May	0.0505	0.0702	0.0197	CFP	F	TT	2-Jun	Borer released from hand rather than placed on stick
35C*	24-May	0.0505	0.0702	0.0197	CFP	F	TT	2-Jun	Borer released from hand rather than placed on stick
35D*	24-May	0.0505	0.0702	0.0197	CFP	F	TT	2-Jun	Borer released from hand rather than placed on stick
36	24-May	0.0568	0.0681	0.0113	CFP	F	TT	2-Jun	
37	24-May	0.0518	0.0626	0.0108	CFP	F	TT	2-Jun	Level flight only
38	24-May	0.0526	0.0665	0.0140	CFP	F	TT	2-Jun	

39	24-May	0.0433	0.0548	0.0115	CFP	F	TT	2-Jun	
40	23-May	0.0570	0.0649	0.0079	CFP	F	TT	2-Jun	
41	23-May	0.0511	0.0614	0.0103	CFP	F	TT	2-Jun	
42	24-May	0.0509	0.0549	0.0040	CFP	F	TT	2-Jun	
43	24-May	0.0504	0.0558	0.0055	CFP	F	TT	2-Jun	Hovered, then climbed
44A*	24-May	0.0345	0.0407	0.0062	CFP	F	TT	2-Jun	Flew short distance and landed
44B*	24-May	0.0345	0.0407	0.0062	CFP	F	TT	2-Jun	Hovered and crashed
45	23-May	0.0490	0.0571	0.0080	CFP	F	TT	2-Jun	
46	25-May	0.0435	0.0487	0.0052	CFP	F	TT	2-Jun	Leveled off, then up
47	25-May	0.0517	0.0537	0.0019	CFP	F	TT	2-Jun	
48	25-May	0.0505	0.0525	0.0020	CFP	F	TT	2-Jun	
49	25-May	0.0536	0.0572	0.0036	CFP	F	TT	2-Jun	
50	25-May	0.0439	0.0499	0.0060	CFP	F	TT	2-Jun	
51	26-May	0.0464	0.0535	0.0071	CFP	F	TT	2-Jun	
52	26-May	0.0477	0.0545	0.0068	CFP	F	TT	2-Jun	
53	26-May	0.0479	0.0558	0.0080	CFP	F	TT	2-Jun	

54*	26-May	0.0412	0.0446	0.0034	CFP	F	TT	2-Jun	Couldn’t find file
55	26-May	0.0395	0.0485	0.0090	CFP	F	TT	2-Jun	
56	23-May	0.0505	0.0613	0.0108	CFP	F	TT	2-Jun	
57A*	23-May	0.0542	0.0641	0.0099	CFP(?)	F	TT	2-Jun	EAB quickly exited video
57B	23-May	0.0542	0.0641	0.0099	CFP(?)	F	TT	2-Jun	
58	23-May	0.0360	NW		CFP	F		2-Jun	
59	23-May	0.0514	NW		CFP	F		2-Jun	
60*	23-May	0.0504	0.0573	0.0069	CFP	F	TT	2-Jun	No video, drop to floor
61	24-May	0.0463	NW		IL	F		2-Jun	
62	23-May	0.0315	0.0378	0.0063	CFP	F	TT	2-Jun	
63	24-May	0.0476	NW		CFP	F		2-Jun	
64*	24-May	0.0482	0.0573	0.0092	IL	F	TT	2-Jun	No data
65*	23-May	0.0447	0.0476	0.0029	CFP	F	TT	2-Jun	No flight, no video
66	24-May	0.0456	0.0490	0.0034	IL	F	TT	2-Jun	
67*	25-May	0.0354	0.0424	0.0071	CFP	F	TT	2-Jun	Never flew
68*	24-May	0.0411	NW		CFP	M		2-Jun	Fell to ground

69	24-May	0.0200	NW		CFP	M		2-Jun	
70	25-May	0.0282	NW		CFP	M		2-Jun	
71	24-May	0.0475	0.0536	0.0061	CFP	F	TT	2-Jun	Weight added after flight No. 12
72	24-May	0.0365	NW		CFP	M		2-Jun	
73	25-May	0.0185	NW		CFP	M		2-Jun	
74	24-May	0.0383	0.0509	0.0126	CFP	F	TT	2-Jun	Weight added after flight No. 13

Key:

* - Not included in the final plotted data

LOC—Area near Ann Arbor, MI, where infested logs were collected

IL—Island Lakes

CFP—County Farm Parks

NW—No weight

WL—Weight Location

BA—Back of abdomen

TT —Top of thorax

Appendix B—Plan View of Experimental Setup

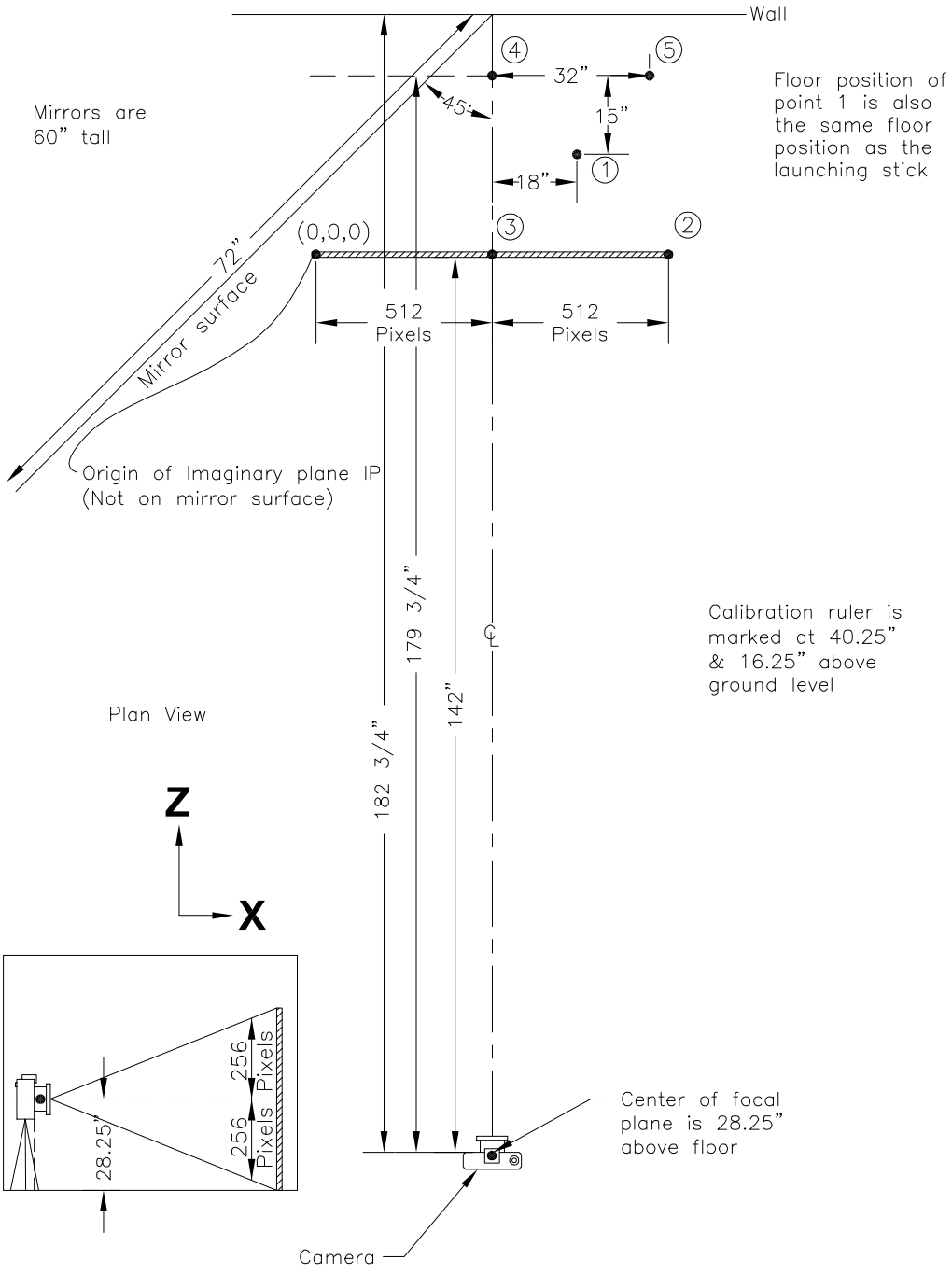

Diagram B.1

Appendix C—Measured Distance From Base of Camera (directly below focal point) to Ruler Calibration Marks

Point #	X (Inches)	Y (Inches)	Z (inches)
1T	18	40.25	164.75 (1)
1B	18	16.25	164.75 (1)
2T	32	40.25	142
2B	32	16.25	142
3T	0	40.25	142
3B	0	16.25	142
4T	0	40.25	179.75
4B	0	16.25	179.75
5T	32	40.25	179.75
5B	32	16.25	179.75
Top of Stick	18	12	164.75 (1)

(1) Derived from 179.75 - 15 = 164.75
T Stands for top mark on calibration ruler.
B Stands for bottom mark on calibration ruler.

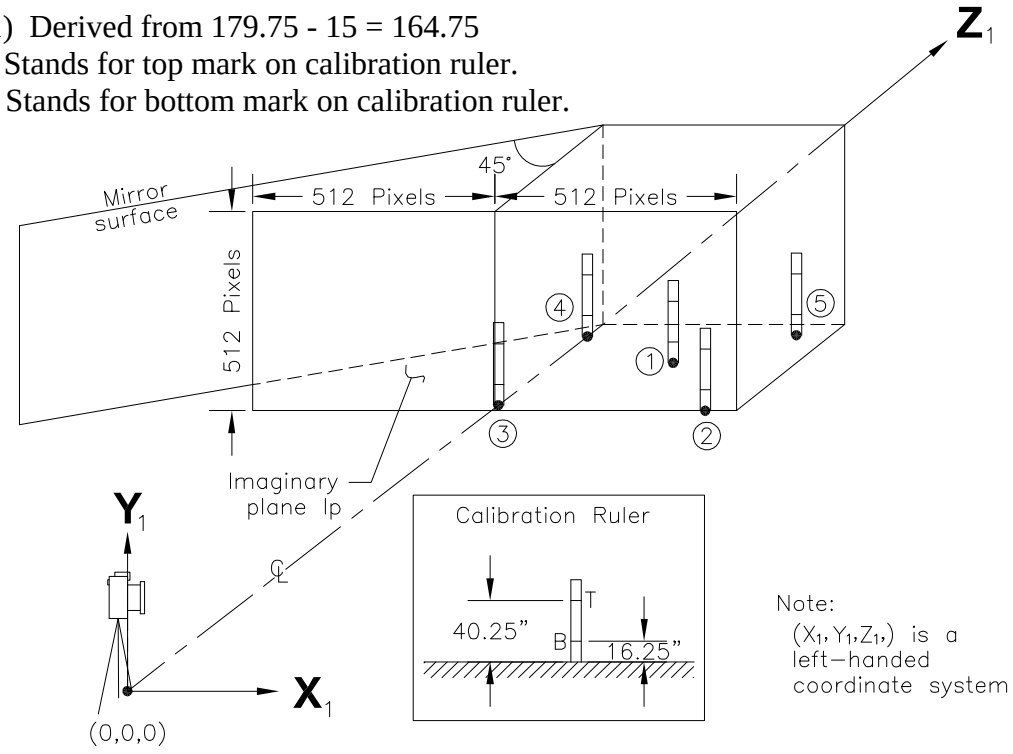

Diagram C.1

Calculation of scale factor on the imaginary plane, *Ip*

- Use calibration point 3.
- Ruler is marked at 16.25 and 40.25 inches
- Distance = 40.25 – 16.25 = 24 inches
- Pixel coordinates are

  3T - 74

  3B - 440
- $SF = \frac{440 - 74}{24} = 15.25$

Appendix D—Videotaped Pixel Locations of Ruler Calibration Marks

Point #	Ref X	Ref Y	X	Y
1T	322	126	749	98
1B	322	384	749	412
2T	107	138	1002	75
2B	107	379	1002	439
3T	39	116	513	74
3B	39	400	513	440
4T	499	114	517	111
4B	480	397	517	399
5T	489	134	898	111
5B	489	375	898	398
Top of Stick	320	430	749	468

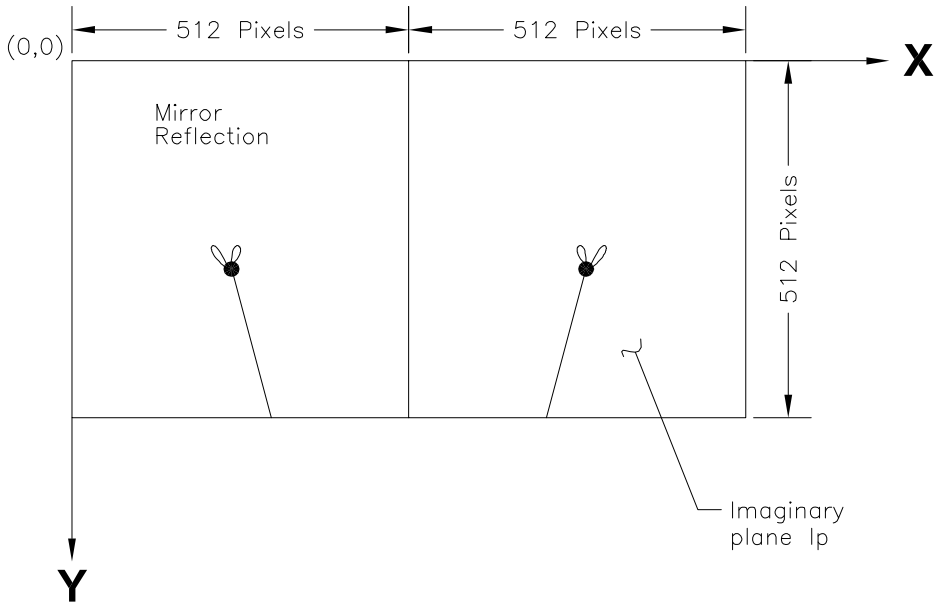

Diagram D.1

Appendix E—Derivation of Transformation Equations

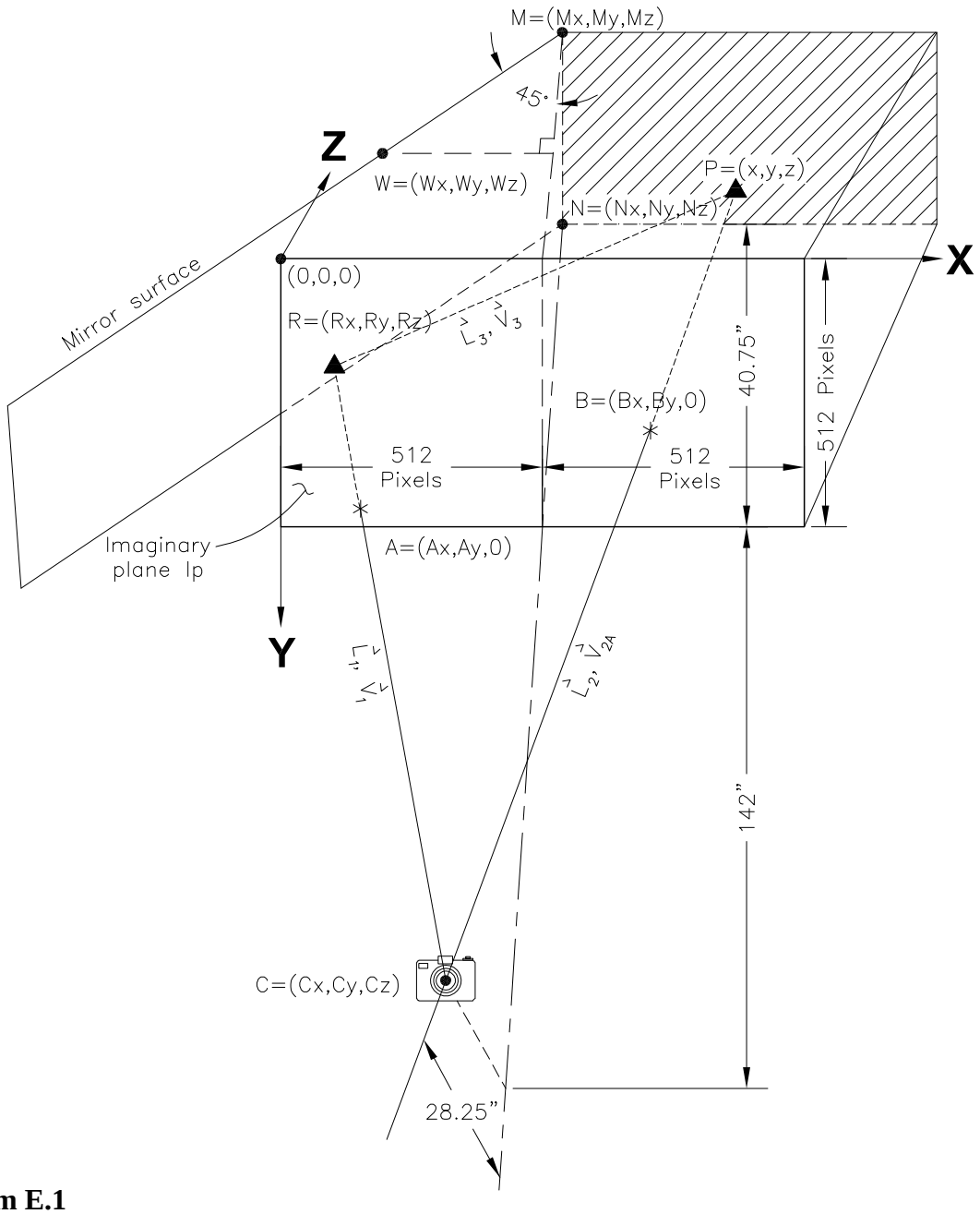

Diagram E.1

Notes:

- Points A & B are on imaginary plane, *Ip*.
- Point R is on surface of mirror.
- Point P is somewhere in the room.

- **Procedure**

1. Find the coordinates of the incident light ray on the mirror by:
    a. Determining and using the vector from the camera's focal point through the reflected image to arrive at the formula for the line.
    b. Determining the formula for the mirror's plane.
    c. Solving for the intersection of this line and the mirror's plane.
2. Determine the direction of the reflected light ray.
3. Use the reflected light ray and the point of intersection on the mirror to arrive at a formula for the line passing through the point of intersection and headed back to the borer's position.
4. Determine the formula for a vertical plane that contains both the camera's focal point and the point of the projected position of the object on the imaginary plane, *Ip*.
5. Solve for the intersection of the reflected light ray from the point on the mirror and the plane determined in step 4. These coordinates are the location of the object relative to the origin on the imaginary plane, *Ip*.

SF = Scale factor in pixels per inch on the face of the imaginary plane, *Ip*.
The default scale factor is 15.25 pixels per inch (see appendix C).

Physical Location of Points Shown on Diagram E.1

$C_X = \frac{512}{SF}$

$C_Y = \frac{256}{SF}$

$C_Z = -142$

$N_X = \frac{512}{SF}$

$N_Y = \frac{512}{SF}$

$N_Z = 40.75$

$M_X = \frac{512}{SF}$

$M_Y = 0$

$M_Z = 40.75$

$W_X = \frac{512}{SF} - 10$

$W_Y = 0$

$W_Z = 30.75$

Step 1.a

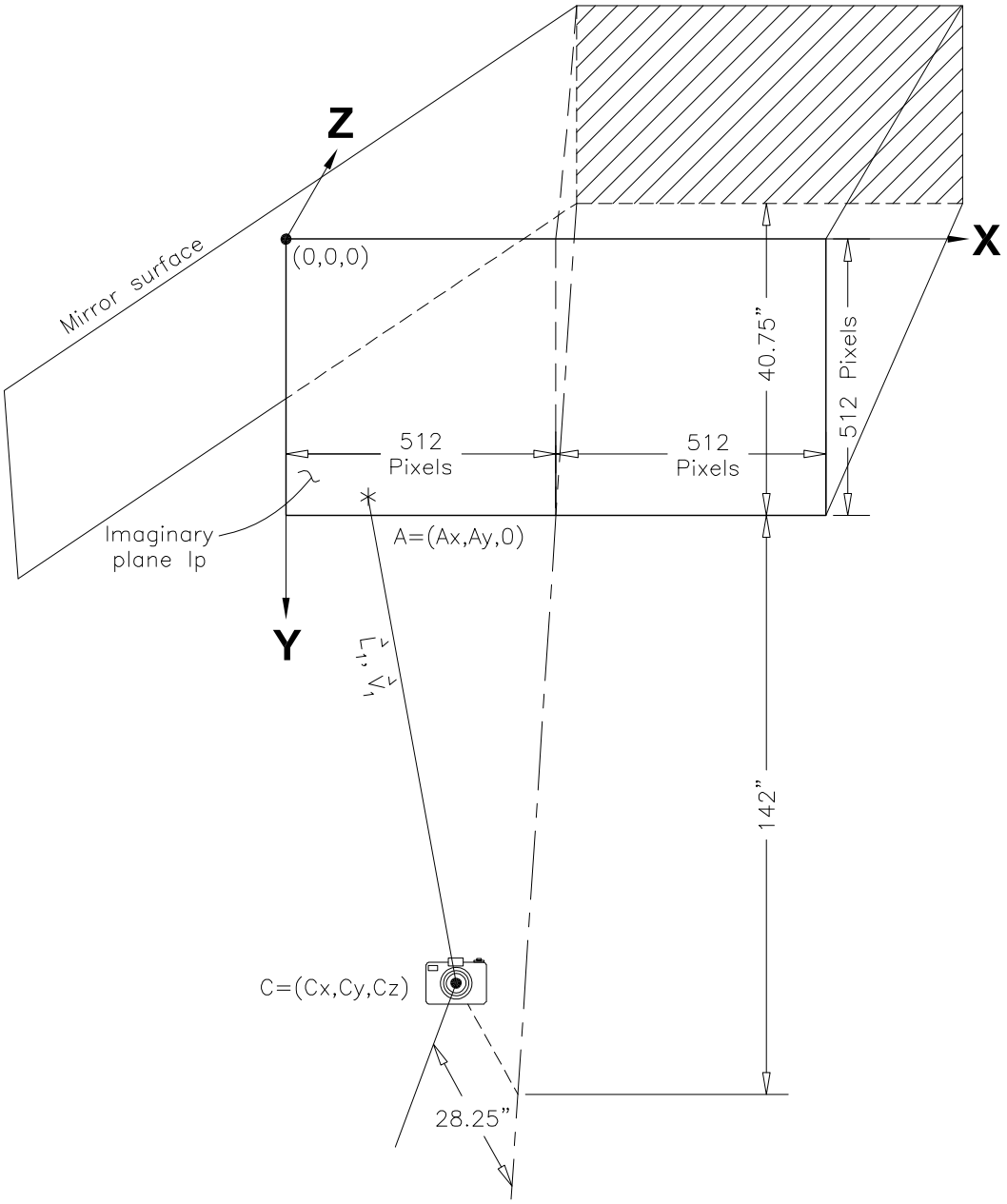

Diagram E.1.a

Note: Vectors will be denoted by a bar over the top of the letter, example: $\overline{V}$ or $\overline{MN}$

Equation formula for line L_1 using a point and direction vector:

Point $\langle C_X, C_Y, C_Z \rangle$
Direction vector $\overline{V_1} = \langle C_X - A_X, C_Y - A_Y, C_Z - 0 \rangle$

Symmetric equations $\dfrac{X - C_X}{C_X - A_X} = \dfrac{Y - C_Y}{C_Y - A_Y} = \dfrac{Z - C_Z}{C_Z}$

Y and Z in terms of X

$$Y = \left(\frac{X - C_X}{C_X - A_X} \right)(C_Y - A_Y) + C_Y \quad \textbf{(Eq. 1.a.1)}$$

$$Z = \left(\frac{X - C_X}{C_X - A_X} \right)(C_Z) + C_Z \quad \textbf{(Eq. 1.a.2)}$$

Step 1.b

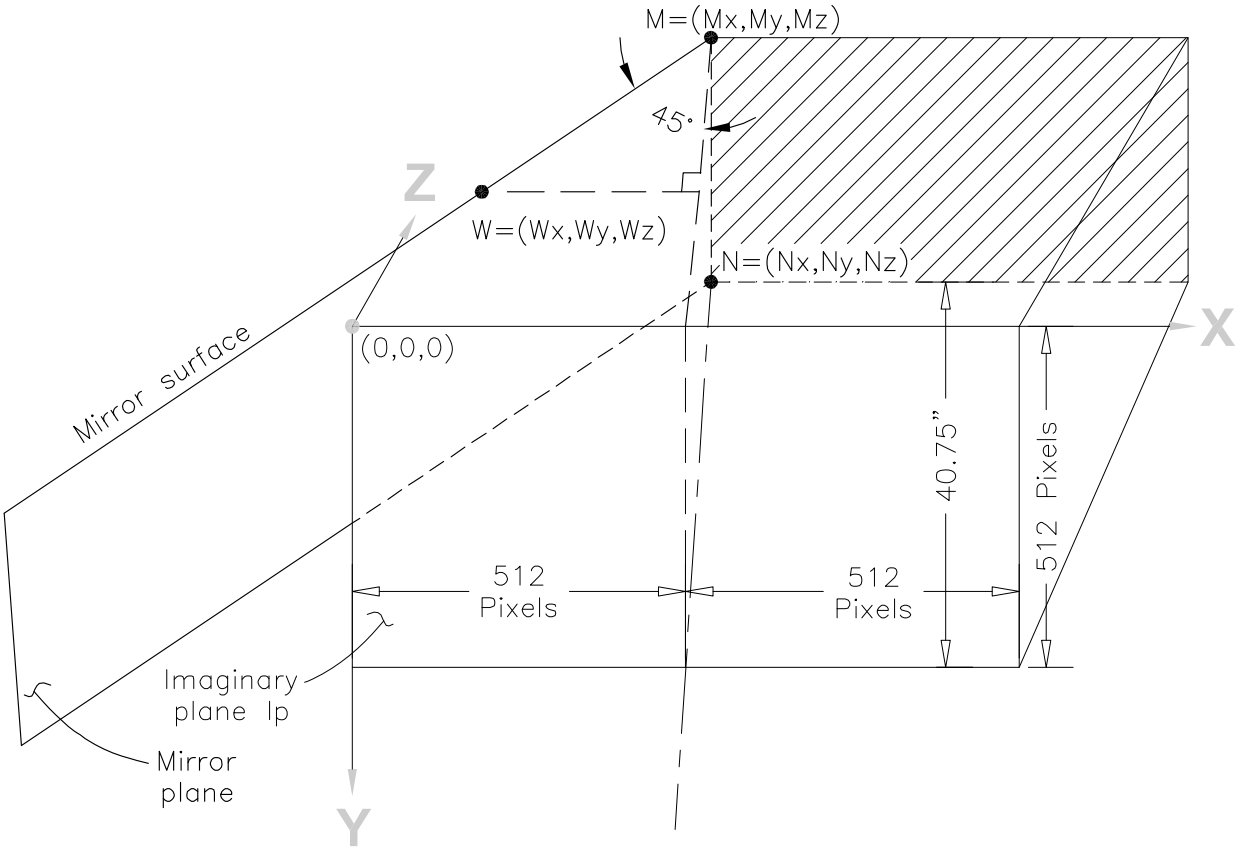

Diagram E.1.b

Equation for the mirror's plane

$$\overline{MN} = \left(\frac{512}{SF} - \frac{512}{SF}\right)\hat{i} + \left(\frac{512}{SF} - 0\right)\hat{j} + (40.75 - 40.75)\hat{k} = \frac{512}{SF}\hat{j}$$

$$\overline{MW} = \left[\left(\frac{512}{SF} - 10\right) - \frac{512}{SF}\right]\hat{i} + (0 - 0)\hat{j} + (30.75 - 40.75)\hat{k} = -10\hat{i} - 10\hat{k}$$

$$\overline{MW} \times \overline{MN} = \begin{vmatrix} i & j & k \\ -10 & 0 & -10 \\ 0 & \frac{512}{SF} & 0 \end{vmatrix} = 10\left(\frac{512}{SF}\right)\hat{i} - 10\left(\frac{512}{SF}\right)\hat{k}$$ Normal to the mirror's plane

Choose point on the mirror's plane $(M_X, M_Y, M_Z) = \left(\frac{512}{SF}, 0, 40.75\right)$

The mirror's plane has an equation in the form of

$$10\left(\frac{512}{SF}\right)X - 10\left(\frac{512}{SF}\right)Z = D$$

$$D = 10\left(\frac{512}{SF}\right)\left(\frac{512}{SF}\right) - 10\left(\frac{512}{SF}\right)(40.75)$$

$$D = 10\left(\frac{512}{SF}\right)\left(\frac{512}{SF} - 40.75\right)$$

The equation of the mirror's plane

$$10\left(\frac{512}{SF}\right)X - 10\left(\frac{512}{SF}\right)Z = 10\left(\frac{512}{SF}\right)\left(\frac{512}{SF} - 40.75\right)$$

$$X - Z = \left(\frac{512}{SF} - 40.75\right) \quad \textbf{(Eq. 1.b)}$$

Step 1.c

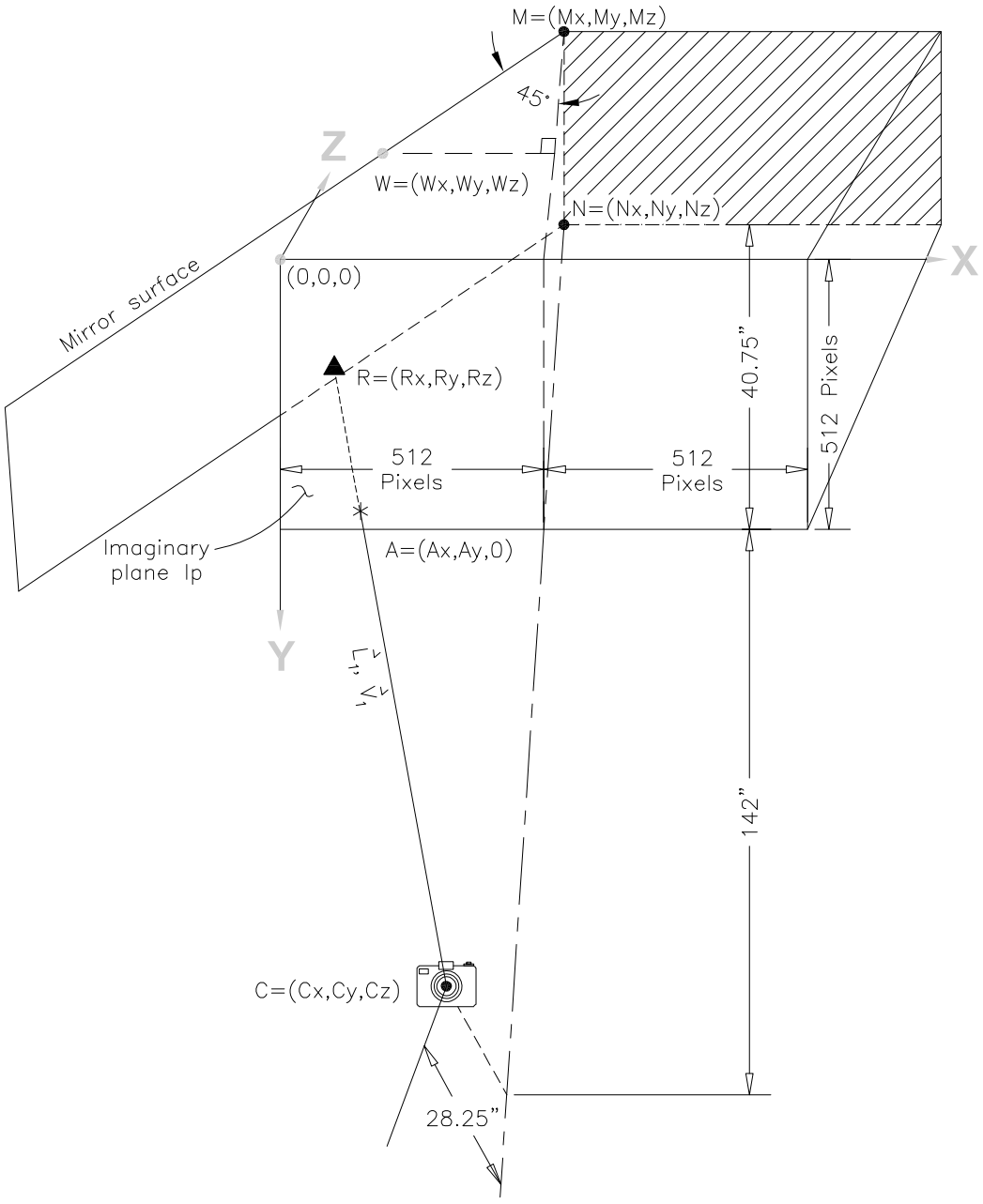

Diagram E.1.c

Insert the symmetric equation (Eq. 1.a.2) into the mirror's plane equation (Eq. 1.b) to get the intersection points on the mirror's plane

$$X - \left[\left(\frac{X - C_X}{C_X - A_X}\right)(C_Z) + C_Z\right] = \left(\frac{512}{SF} - 40.75\right)$$

$$X - \left(\frac{X - C_X}{C_X - A_X}\right)(C_Z) - C_Z - \frac{512}{SF} + 40.75 = 0$$

$$X(C_X - A_X) - C_Z(X - C_X) - C_Z(C_X - A_X) - \frac{512}{SF}(C_X - A_X) + 40.75(C_X - A_X) = 0$$

$$XC_X - XA_X - XC_Z + C_ZC_X - C_ZC_X + C_ZA_X - C_X\frac{512}{SF} + \frac{512}{SF}A_X + 40.75C_X - 40.76A_X = 0$$

$$X(C_X - A_X - C_Z) + C_X\left(40.75 - \frac{512}{SF}\right) + A_X\left(C_Z - 40.75 + \frac{512}{SF}\right) = 0$$

$$X = \frac{A_X\left(40.75 - C_Z - \frac{512}{SF}\right) + C_X\left(\frac{512}{SF} - 40.75\right)}{(C_X - A_X - C_Z)}$$

$$X = \frac{A_X\left(40.75 + 142 - \frac{512}{SF}\right) + \frac{512}{SF}\left(\frac{512}{SF} - 40.75\right)}{\left(\frac{512}{SF} - A_X + 142\right)}$$

$$R_X = X = \frac{A_X\left(182.75 - \frac{512}{SF}\right) + \frac{512}{SF}\left(\frac{512}{SF} - 40.75\right)}{\left(\frac{512}{SF} + 142 - A_X\right)} \qquad \textbf{(Eq. 1.c.1)}$$

Back substitute equation 1.c.1 into equation 1.a.1 to get R_Y

$$R_Y = Y = \left(\frac{R_X - C_X}{C_X - A_X}\right)(C_Y - A_Y) + C_Y$$

$$R_Y = \left(\frac{R_X - \frac{512}{SF}}{\frac{512}{SF} - A_X}\right)\left(\frac{256}{SF} - A_Y\right) + \frac{256}{SF} \qquad \textbf{(Eq. 1.c.2)}$$

Back substitute equation 1.c.1 into equation 1.a.2 to get R_Z

$$R_Z = Z = \left(\frac{R_X - C_X}{C_X - A_X} \right)(C_Z) + C_Z$$

$$R_Z = \left[\left(\frac{R_X - \frac{512}{SF}}{\frac{512}{SF} - A_X} \right)(-142) - 142 \right] \qquad \textbf{(Eq. 1.c.3)}$$

Step 2

Once the mirror intersection point (R_X, R_Y, R_Z) is found on the mirror's plane, determine the equation for the reflected line.

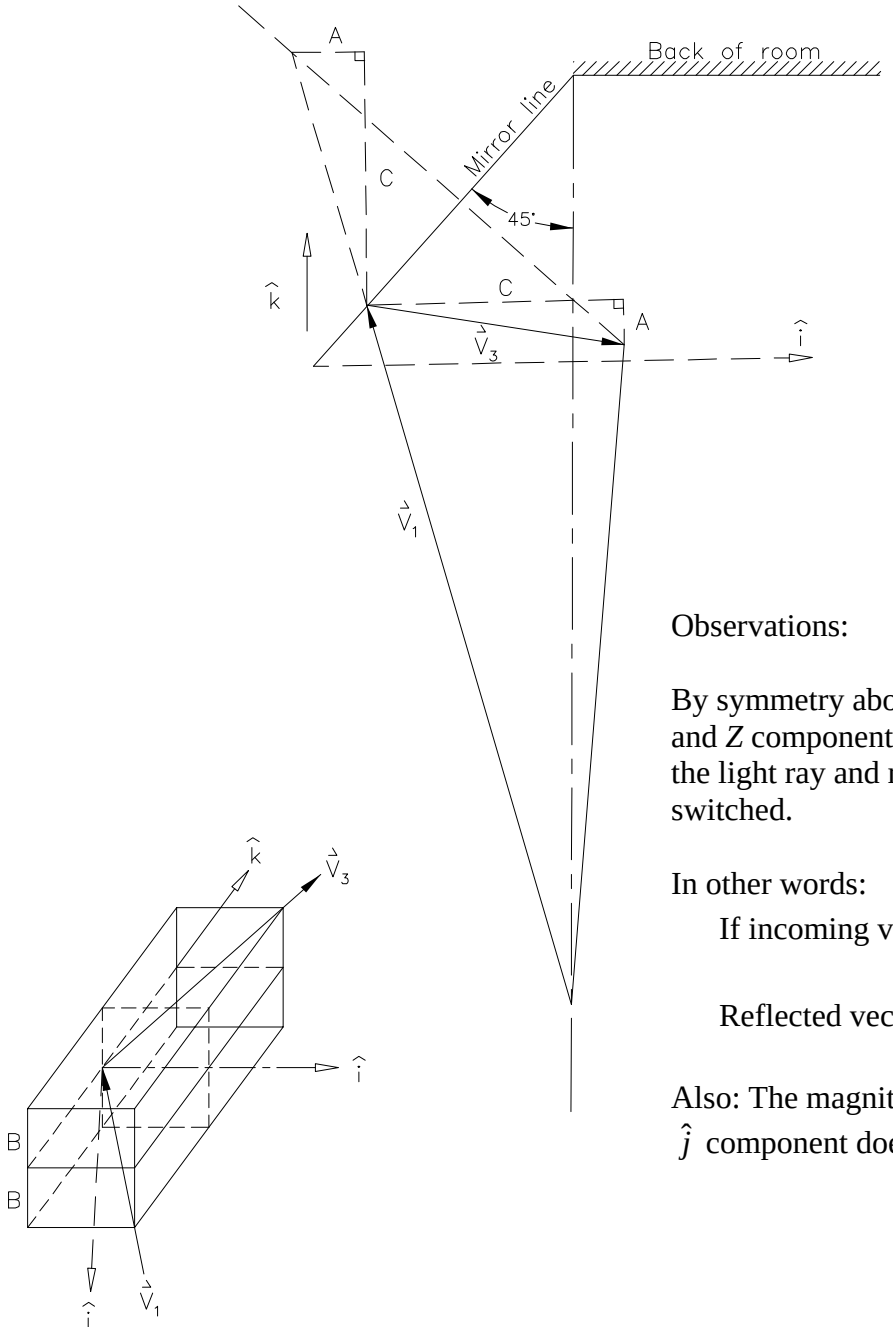

Diagram E.2

Observations:

By symmetry about the mirror line, the *X* and *Z* components of directional vectors for the light ray and reflected light ray are switched.

In other words:

If incoming vector $\vec{V}_1 = -A\hat{i} + B\hat{j} + C\hat{k}$

Reflected vector $\vec{V}_3 = C\hat{i} + B\hat{j} - A\hat{k}$

Also: The magnitude and direction of the $\hat{j}$ component doesn't change.

Incoming vector $\vec{V}_1$

$$\vec{V}_1 = \langle A_X - C_X\,,\, A_Y - C_Y\,,\, 0 - C_Z \rangle$$

or

$$\left(A_X - \frac{512}{SF}\right)\hat{i} + \left(A_Y - \frac{256}{SF}\right)\hat{j} + (142)\hat{k}$$

Therefore the reflected vector is

$$142\hat{i} + \left(A_Y - \frac{256}{SF}\right)\hat{j} + \left(A_X - \frac{512}{SF}\right)\hat{k}$$

or

$$\vec{V}_3 = \left\langle 142, A_Y - \frac{256}{SF}, A_X - \frac{512}{SF} \right\rangle$$

Step 3

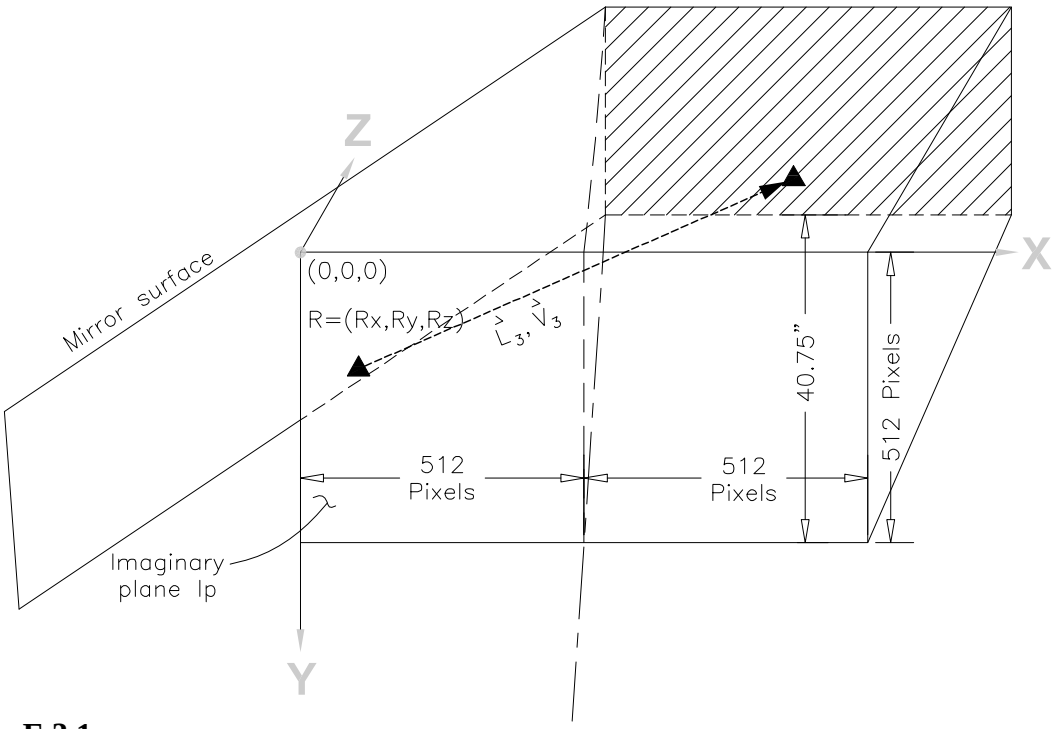

Diagram E.3.1

The general form of symmetric equations for the line L_3 with this directional vector running through point (R_x, R_y, R_z) is

General form: $\frac{X - X_0}{V_X} = \frac{Y - Y_0}{V_Y} = \frac{Z - Z_0}{V_Z}$

or: $\frac{X - R_X}{142} = \frac{Y - R_Y}{A_Y - \frac{256}{SF}} = \frac{Z - R_Z}{A_X - \frac{512}{SF}}$

Redefine symmetric equations using the following variables:

$A = 142$ **(Eq. 3.1)**

$B = A_Y - \frac{256}{SF}$ **(Eq. 3.2)**

$C = A_X - \frac{512}{SF}$ **(Eq. 3.3)**

$\frac{X - R_X}{A} = \frac{Y - R_Y}{B} = \frac{Z - R_Z}{C}$

Step 4

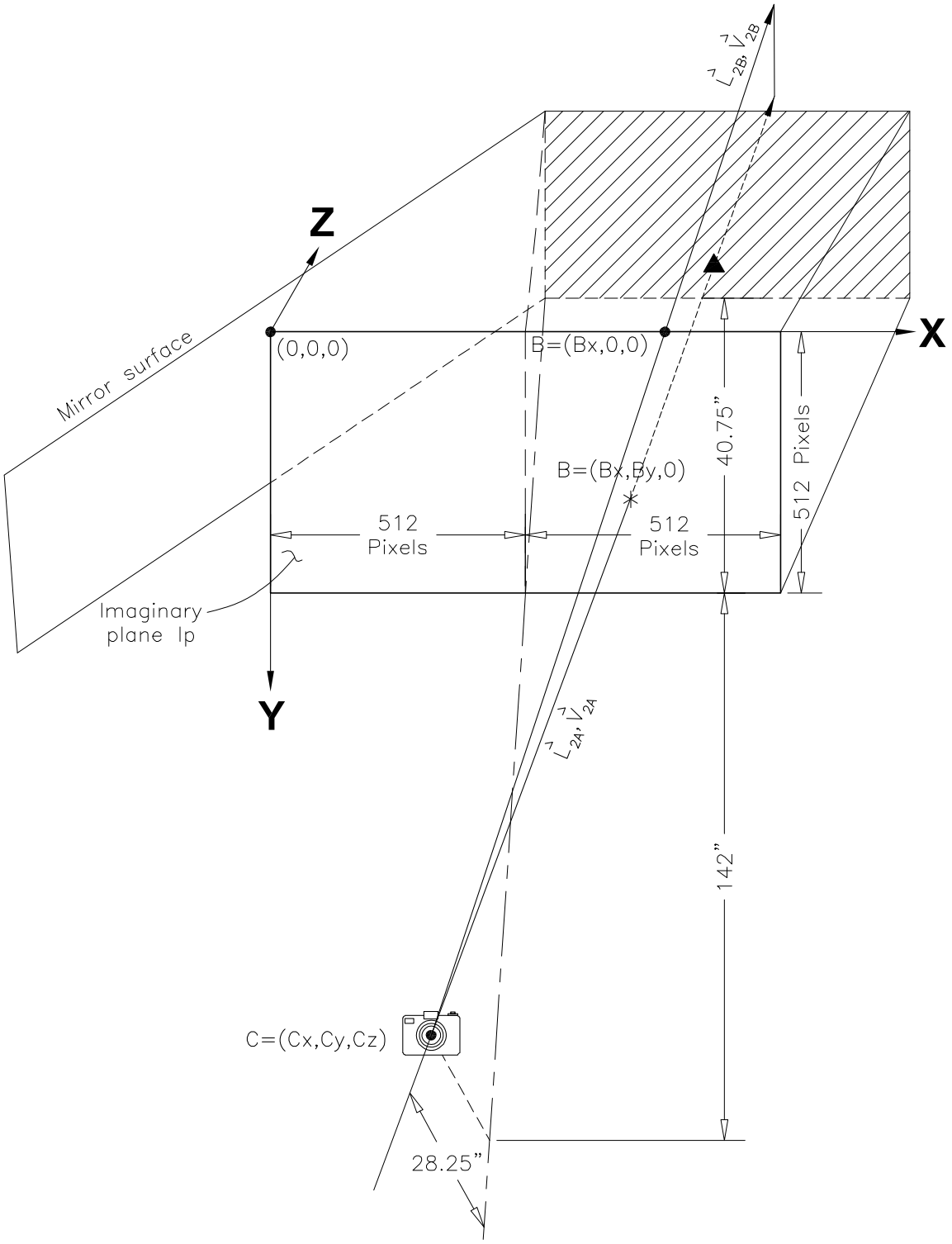

Diagram E.4.1

Find the vertical plane that lies on lines L_{2A} and L_{2B}.

Directional vectors for $L_{2A} = \vec{V}_{2A} = \langle B_X - C_X, B_Y - C_Y, 0 - C_Z \rangle$

$$\vec{V}_{2A} = \left\langle B_X - \frac{512}{SF}, B_Y - \frac{256}{SF}, 142 \right\rangle$$

Another line L_{2B} in that vertical plane would be from the camera through point $(B_X, 0, 0)$.

$$\vec{V}_{2B} = \left\langle B_X - \frac{512}{SF}, 0 - \frac{256}{SF}, 142 \right\rangle$$

A normal vector to this plane would be $\vec{V}_{2A} \times \vec{V}_{2B}$.

$$\vec{V}_{2A} \times \vec{V}_{2B} = \begin{vmatrix} \hat{i} & \hat{j} & \hat{k} \\ B_X - \frac{512}{SF} & B_Y - \frac{256}{SF} & 142 \\ B_X - \frac{512}{SF} & -\frac{256}{SF} & 142 \end{vmatrix}$$

$$\vec{V}_{2A} \times \vec{V}_{2B} = \left[\left(B_Y - \frac{256}{SF} \right) 142 - 142 \left(-\frac{256}{SF} \right) \right] \hat{i}$$
$$+ \left[\left(B_X - \frac{512}{SF} \right) 142 - 142 \left(B_X - \frac{512}{SF} \right) \right] \hat{j}$$
$$+ \left[\left(B_X - \frac{512}{SF} \right) \left(-\frac{256}{SF} \right) - \left(B_X - \frac{512}{SF} \right) \left(B_Y - \frac{256}{SF} \right) \right] \hat{k}$$

Simplify $\hat{i}, \hat{j}, \hat{k}$ components of vector

$$142 B_Y - 142 \left(\frac{256}{SF} \right) + 142 \left(\frac{256}{SF} \right) = 142 B_Y \hat{i}$$

$$\left[\left(B_X - \frac{512}{SF} \right) 142 - 142 \left(B_X - \frac{512}{SF} \right) \right] \hat{j} = 0 \hat{j}$$

$$\frac{-256}{SF} B_X + \left(\frac{512}{SF} \right) \left(\frac{256}{SF} \right) - B_X B_Y + B_X \left(\frac{256}{SF} \right) + B_Y \left(\frac{512}{SF} \right) - \left(\frac{512}{SF} \right) \left(\frac{256}{SF} \right)$$

$$= -B_X B_Y + B_Y \left(\frac{512}{SF} \right) \hat{k}$$

$$= B_Y \left(\frac{512}{SF} - B_X \right) \hat{k}$$

The full equation for this plane is in the form

$$142B_Y X + B_Y\left(\frac{512}{SF} - B_X\right)Z = D$$

Since the vertical plane also runs through point $(B_X, 0, 0)$

$$D = 142B_Y(B_X) + B_Y\left(\frac{512}{SF} - B_X\right)(0)$$

$$D = 142B_X B_Y$$

The full equation for the vertical plane containing the camera's focal point and the borer is:

$$142B_Y X + B_Y\left(\frac{512}{SF} - B_X\right)Z = 142B_X B_Y$$

$$142X + \left(\frac{512}{SF} - B_X\right)Z = 142B_X \qquad \textbf{(Eq. 4.1)}$$

Step 5

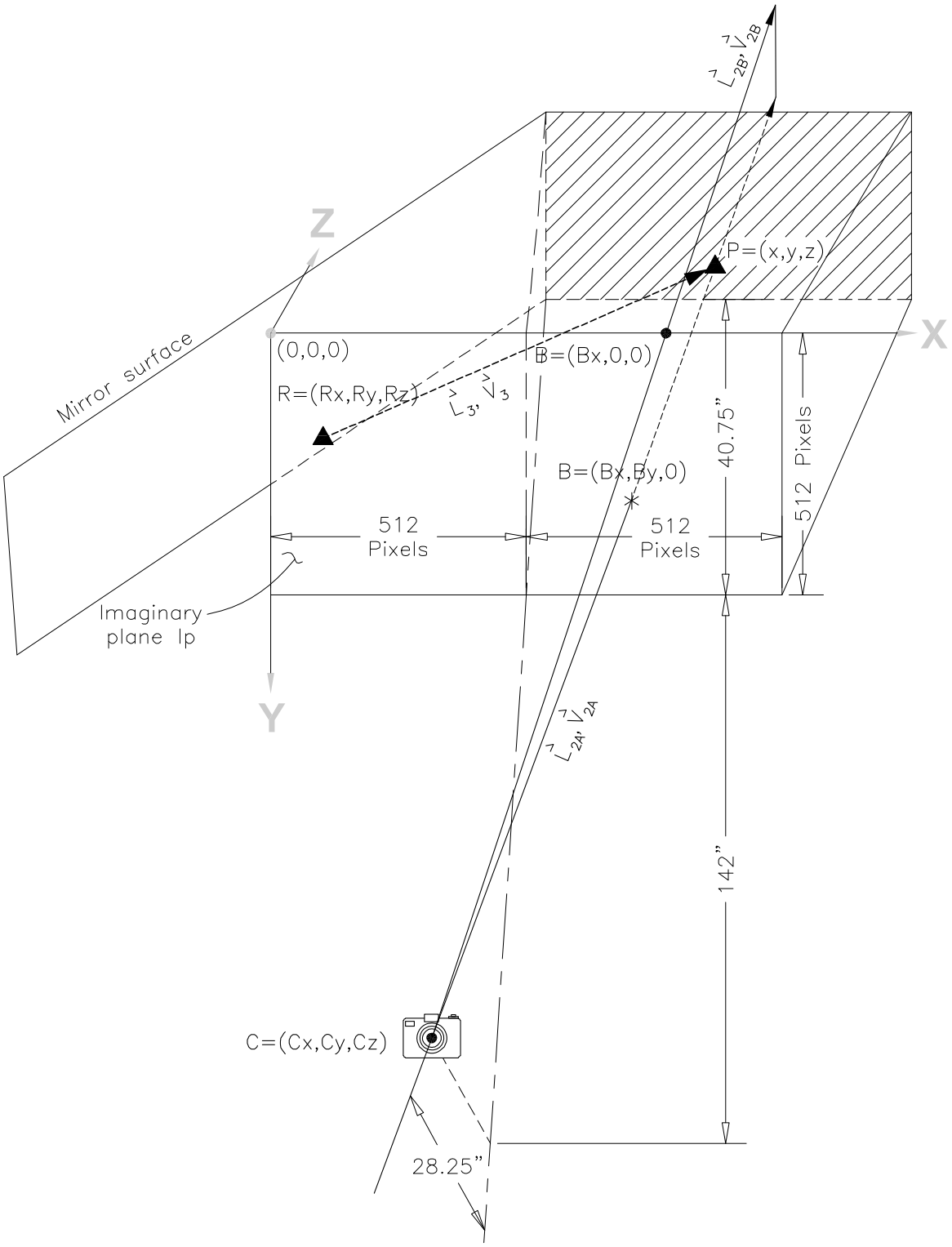

Diagram E.5.1

The reflected line off the mirror surface, L_3, will intersect the vertical plane containing the borer.

$$142X + \left(\frac{512}{SF} - B_X\right)\left[\left(\frac{X - R_X}{A}C\right) + R_Z\right] = 142B_X$$

$$142X + \left(\frac{512}{SF} - B_X\right)\left(\frac{XC - R_XC + AR_Z}{A}\right) - 142B_X = 0$$

$$142AX + \left(\frac{512}{SF} - B_X\right)\left(XC - R_XC + AR_Z\right) - 142AB_X = 0$$

$$142AX + \frac{512}{SF}XC - \frac{512}{SF}R_XC + \frac{512}{SF}AR_Z - B_XCX + B_XR_XC - AB_XR_Z - 142AB_X = 0$$

$$X\left(142A + \frac{512}{SF}C - B_XC\right) + CR_X\left(B_X - \frac{512}{SF}\right) + A\left(\frac{512}{SF}R_Z - B_XR_Z - 142B_X\right) = 0$$

Final Transformation Equations

$$X = \frac{CR_X\left(\frac{512}{SF} - B_X\right) + A\left(142B_X + B_XR_Z - \frac{512}{SF}R_Z\right)}{\left(142A + \frac{512}{SF}C - B_XC\right)} \quad \textbf{(Eq. 5.1)}$$

$$Y = \frac{(X - R_X)B}{A} + R_Y \quad \textbf{(Eq. 5.2)}$$

$$Z = \frac{(X - R_X)C}{A} + R_Z \quad \textbf{(Eq. 5.3)}$$

Repeating equations 3.1 to 3.3

$$A = 142$$

$$B = A_Y - \frac{256}{SF}$$

$$C = A_X - \frac{512}{SF}$$

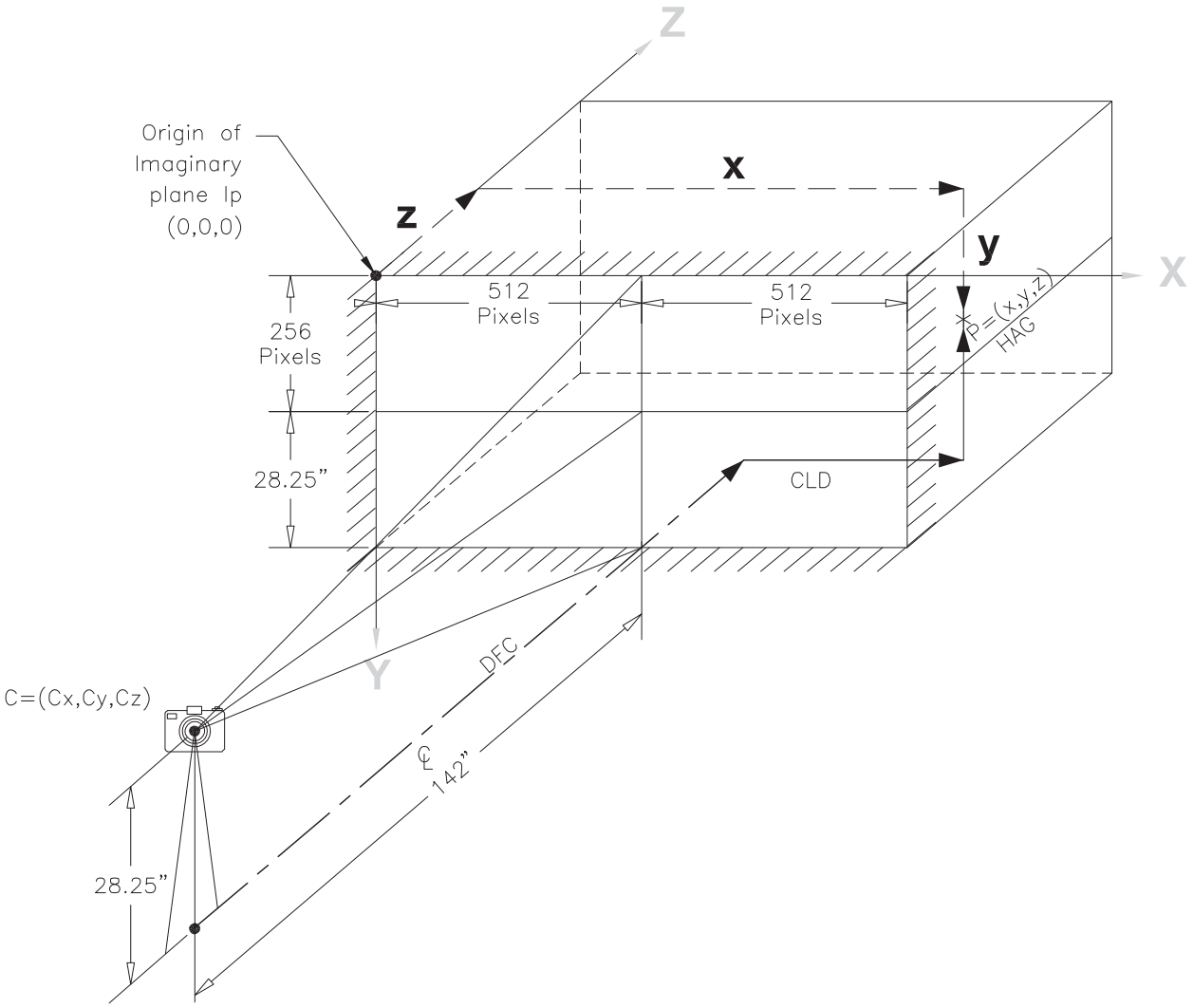

Diagram E.6

Important concepts: SF- Scale Factor – 15.25 pixels per inch

- Location of focal point C in relation to imaginary plane origin is given as
  $(C_X, C_Y, C_Z) = \left(\frac{512}{SF}, \frac{256}{SF}, -142\right)$
- All derived locations are based on these coordinate relationships.
- When actual object locations are desired in relation to the camera's base projected on the floor below its focal point:
  1. $\frac{512}{SF}$ must be subtracted from *x* dimension to get centerline distance (CLD)
  2. 142 inches must be added to the *z* dimension to get the distance from camera (DFC)
  3. The calculated *y* coordinate must be subtracted from $\frac{256}{SF} + 28.25$ inches to get the object height above ground (HAG).

Appendix F—Determination of Percent Error

x and y are the object's actual pixel coordinates.
X-ref and Y-ref are the object's reflected pixel coordinates.

Point	X-ref (Pixel)	Y-ref (Pixel)	*x* (Pixel)	*y* (Pixel)	Scale factor	*Ax* (Inches)	*Ay* (Inches)	*Bx* (Inches)	*By* (Inches)	*Rx* (Inches)	*Ry* (Inches)	*Rz* (Inches)
1T	322	126	749	98	15.25	21.11475	8.262295	49.11475	6.42623	18.83274	6.700916	26.00897
1B	322	384	749	412	15.25	21.11475	25.18033	49.11475	27.01639	18.83274	26.71769	26.00897
2T	107	138	1002	75	15.25	7.016393	9.04918	65.70492	4.918033	4.780248	8.397661	11.95648
2B	107	379	1002	439	15.25	7.016393	24.85246	65.70492	28.78689	4.780248	25.53158	11.95648
3T	39	116	513	74	15.25	2.557377	7.606557	33.63934	4.852459	0.812448	7.090088	7.988677
3B	39	400	513	440	15.25	2.557377	26.22951	33.63934	28.85246	0.812448	26.76073	7.988677
4T	499	114	517	111	15.25	32.72131	7.47541	33.90164	7.278689	32.48323	4.87479	39.65946
4B	480	397	517	399	15.25	31.47541	26.03279	33.90164	26.16393	30.91256	28.51282	38.08879
5T	489	134	898	111	15.25	32.06557	8.786885	58.88525	7.278689	31.65316	6.599314	38.82939
5B	489	375	898	398	15.25	32.06557	24.59016	58.88525	26.09836	31.65316	26.72394	38.82939
Top of calibration stick	320	430	749	468	15.25	20.98361	28.19672	49.11475	30.68852	18.69021	30.27511	25.86644

Analysis Approach:
Scale factor (SF) is derived from the pixel-to-actual-height ratio taken at ruler calibration point 3. "T" stands for "Top." "B" stands for "Bottom."
Vertical calibration marks are at 40.25 inches (pixel coordinate 75) and 16.25 inches (pixel coordinate 439).
Therefore SF = (440 - 74)/(40.25 - 16.25) = 15.25

The *x*, *y*, *z* coordinates are in relation to the origin of the common plane, *Ip*.
The relative differences in *x*, *y*, *z* coordinates are used to determine the incremental change in the borer's position.
The time code on the video is synchronized to the digitized position and used to calculate the incremental average speed of the borer.

To determine the borer's location from the camera's focal point:
CLD—Centerline Distance
CLD: 512/SF or 512/15.25 = 33.57377 inches must be subtracted from the calculated *x* coordinate.

DFC—Distance from Camera
DFC: 142 inches must be added to the calculated *Z* coordinate.

HAG—Height Above Ground

HAG: The calculated *y* coordinate must be subtracted from 256/SF or 256/15.25 = 16.786 inches and then added to 28.25 inches.

The accuracies of positions are determined by comparing calculated positions of points on a calibration ruler from the camera's focal point to measured distances.

a	***b***	***c***	***X_1***	***X_2***	***X_3***	***X***	***Y***	***Z***	**CLD**	**HAG**	**DFC**
142	-8.52459	-12.459	3646.496	1047747	20357.63	51.64618	4.731049	23.12993	18.07241	40.30584	165.1299
142	8.393443	-12.459	3646.496	1047747	20357.63	51.64618	28.65725	23.12993	18.07241	16.37964	165.1299
142	-7.7377	-26.5574	4079.076	1379427	21017.32	65.82695	5.071173	0.539293	32.25318	39.96571	142.5393
142	8.065574	-26.5574	4079.076	1379427	21017.32	65.82695	28.99903	0.539293	32.25318	16.03786	142.5393
142	-9.18033	-31.0164	1.652407	678378.1	20166.03	33.63972	4.967798	0.81837	0.065952	40.06909	142.8184
142	9.442623	-31.0164	1.652407	678378.1	20166.03	33.63972	28.94366	0.81837	0.065952	16.09322	142.8184
142	-9.31148	-0.85246	9.078892	685439.1	20164.28	33.99319	4.775776	39.65039	0.419419	40.26111	181.6504
142	9.245902	-2.09836	21.26745	685366	20164.69	33.98948	28.71317	38.04333	0.415708	16.32372	180.0433
142	-8	-1.5082	1208.349	1326924	20202.17	65.74204	4.678814	38.46733	32.16827	40.35807	180.4673
142	7.803279	-1.5082	1208.349	1326924	20202.17	65.74204	28.59722	38.46733	32.16827	16.43967	180.4673
142	11.40984	-12.5902	3656.992	1047432	20359.66	51.62607	32.92154	22.94624	18.0523	12.11534	164.9462

Diff	Diff	Diff	% diff	% diff	% diff	% diff Dist from Focal
CLD	**HAG**	**DFC**	**CLD**	**HAG**	**DFC**	
0.072405	0.055836	0.379932	0.402252	0.138723	0.230611	0.2274092
0.072405	0.129638	0.379932	0.402252	0.797775	0.230611	0.2380342
0.253176	-0.28429	0.539293	0.791176	0.706305	0.379784	0.1455356
0.253176	-0.21214	0.539293	0.791176	1.305481	0.379784	0.378891
0.065952	-0.18091	0.81837	6.595168	0.449473	0.576317	0.5004
0.065952	-0.15678	0.81837	6.595168	0.964771	0.576317	0.5565572
0.419419	0.011109	1.900391	41.94191	0.027601	1.057241	1.0085744
0.415708	0.073717	0.293326	41.57084	0.453646	0.163186	0.1658083
0.16827	0.108072	0.717331	0.525845	0.268501	0.399071	0.3967398
0.16827	0.189668	0.717331	0.525845	1.167187	0.399071	0.4089972
0.052302	0.115343	0.19624	0.290564	0.961189	0.119114	0.1255376

Appendix G—Calculated Results for Plotting—(Using Combined Hatch Dates)

Flight No.	Borer weight (milligrams)	Load weight (milligrams)	Percent of body weight	Flight time (seconds)	Speed (feet per second)
Females					
1	35.34	0	0.00	0.62	4.08
5	43.63	0	0.00	0.64	4.41
6	52.91	0	0.00	1.09	3.87
8	33.22	0	0.00	1.12	3.52
9	42.79	0	0.00	0.77	4.49
10	36.32	0	0.00	0.99	4.05
12	44.55	0	0.00	0.98	4.08
13	41.04	0	0.00	0.88	4.86
14	53	0	0.00	0.65	4.28
15	33.96	0	0.00	0.84	4.35
16	40.63	0	0.00	0.75	4.76
18	46.86	0	0.00	1.12	3.75
19	53.15	0	0.00	1.20	3.99
20	49	2.45	5.00	1.14	4.03
22	27.17	2.12	7.03	1.56	3.37
25	33.31	0.99	2.97	0.68	4.05
26_25A	45.48	1.05	2.31	1.46	3.72

27	44.91	3.37	7.50	1.36	3.22
29	38.61	8.35	21.63	1.40	3.18
30	45.94	9.84	21.42	1.24	3.85
31A	44.25	13.33	30.12	1.36	2.97
32	45.93	13.33	29.02	1.31	2.92
34	42.41	15.99	37.70	1.08	2.84
36	56.83	11.25	19.80	0.82	2.58
37	51.79	10.78	20.81	1.92	3.06
38	52.56	13.98	26.60	1.04	3.24
39	43.31	11.46	26.46	1.11	3.49
40	56.97	7.89	13.85	0.92	3.82
41	51.11	10.3	20.15	2.06	2.51
42A	50.85	4.02	7.91	0.97	3.99
43	50.38	5.46	10.84	1.57	3.46
45	49.04	8.02	16.35	1.10	3.56
46	43.49	5.2	11.96	1.13	4.55
47	51.73	1.92	3.71	0.93	4.40
48	50.54	2	3.96	1.61	3.42
49	53.59	3.6	6.72	0.74	4.04
50	43.9	6.04	13.76	1.14	3.43
51	46.37	7.13	15.38	1.19	3.22
52	47.71	6.82	14.29	0.90	3.11
53	47.85	7.98	16.68	1.08	3.35

55	39.53	8.96	22.67	1.61	3.71
56	50.51	10.8	21.38	1.26	2.75
57B	54.2	9.86	18.19	1.12	5.41
58	36.02	0	0.00	0.76	4.38
59	51.43	0	0.00	1.39	3.53
61	46.33	0	0.00	0.93	4.10
62	31.51	6.27	19.90	1.55	4.30
63	47.6	0	0.00	1.36	4.19
66	45.62	3.37	7.39	0.82	4.46
71	47.5	6.13	12.91	1.43	3.25
74	38.28	12.61	32.94	1.14	3.51

Males (not included in plotted female data)

69	20.02	0	0.00	1.20	3.96
70	28.21	0	0.00	0.78	4.41
72	36.5	0	0.00	0.81	4.45
73	18.52	0	0.00	0.66	4.40

About the Authors

Keith Windell is a project leader for reforestation, fire, and residues projects. He has a bachelor's degree in mechanical engineering from Montana State University. He has worked for the California Department of Forestry, U.S. Department of the Interior Bureau of Land Management, and the U.S. Department of Agriculture Forest Service.

Jim Kautz retired in 2007 as a photographic technologist for the Missoula Technology and Development Center. He used photographic instrumentation to collect data for various projects with an emphasis on fire projects. He has a bachelor of science degree in photography from Montana State University.

Library Card

Windell, Keith; Kautz, Jim. 2007. Determining how much weight emerald ash borers can carry in flight. Tech Rep. 0734–2815–MTDC. Missoula, MT: U.S. Department of Agriculture Forest Service, Missoula Technology and Development Center. 49 p.

The emerald ash borer (*Agrilus planipennis*), an exotic beetle from Asia, is a recently introduced insect pest. Tiny transponders have been used to track the spread of other introduced insects, but the emerald ash borer is much smaller, weighing just 50 milligrams or so. Female emerald ash borers are larger than male borers, which may be too small to carry a transponder. The heaviest weight a female emerald ash borer could carry in flight was 16 milligrams, 37 percent of her body weight. High-speed cameras showed that the fastest female emerald ash borer flew an average of 5.4 feet per second for 72 inches with a 9.86 milligram load, 18 percent of her body weight.

Key Words: *Agrilus planipennis*, flight, forest health, high speed photography, insects, plant pests, tracking, transponders

For additional information about emerald ash borers, contact Keith Windell at MTDC:
Phone: 406–329–3956
Fax: 406–329–3719
E-mail: *kwindell@fs.fed.us*

Electronic copies of MTDC's documents are available on the Internet at:
http://www.fs.fed.us/eng/t-d.php

Forest Service and Bureau of Land Management employees can search a more complete collection of MTDC's documents, videos, and CDs on their internal computer networks at:
http://fsweb.mtdc.wo.fs.fed.us/search/